

# Explorations of new second-order NLO materials in the K<sup>I</sup>-M<sup>II</sup>-I<sup>V</sup>-O systems

Pei-Xin Li<sup>a,b</sup>, Chun-Li Hu<sup>a</sup>, Xiang Xu<sup>a</sup>, Rui-Yao Wang<sup>c</sup> and Jiang-Gao Mao<sup>a\*</sup>

## Supporting Information

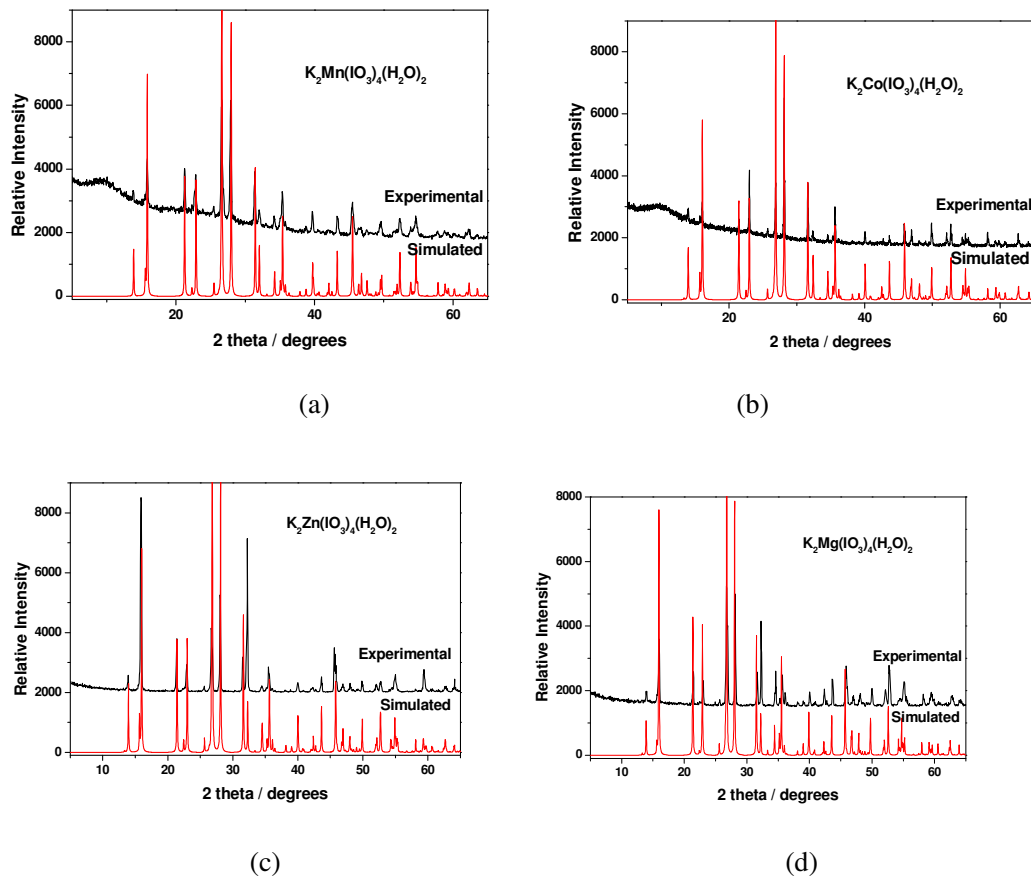


Figure S1. Simulated and experimental XRD powder patterns for  $K_2\text{M}(\text{IO}_3)_4(\text{H}_2\text{O})_2$  ( $\text{M} = \text{Mn}, \text{Co}, \text{Zn}, \text{Mg}$ ).

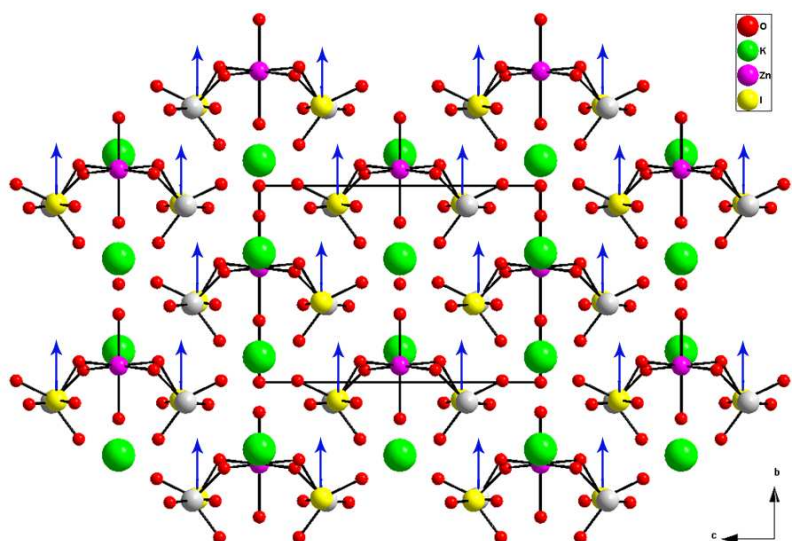


Figure S2. View of the structure of  $\text{K}_2\text{Zn}(\text{IO}_3)_4(\text{H}_2\text{O})_2$  along the  $a$  axis. K, Zn, I(1), I(2) and O atoms are represented by green, pink, yellow, light grey and red circles, respectively. The polarization directions of the iodate groups are indicated by green arrows.

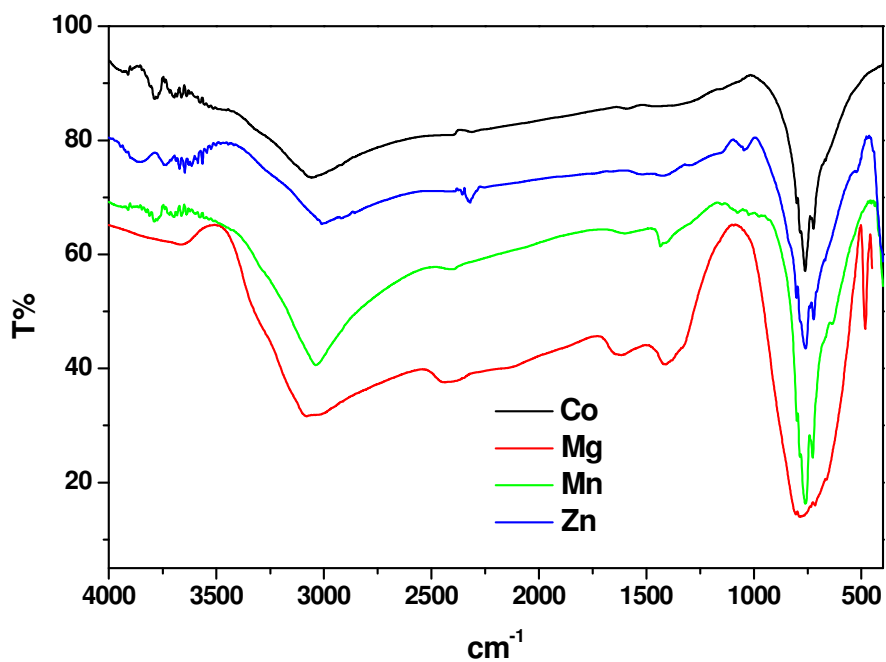


Figure S3. IR diagrams for  $\text{K}_2\text{M}(\text{IO}_3)_4(\text{H}_2\text{O})_2$  ( $\text{M} = \text{Mn}, \text{Co}, \text{Zn}, \text{Mg}$ ).

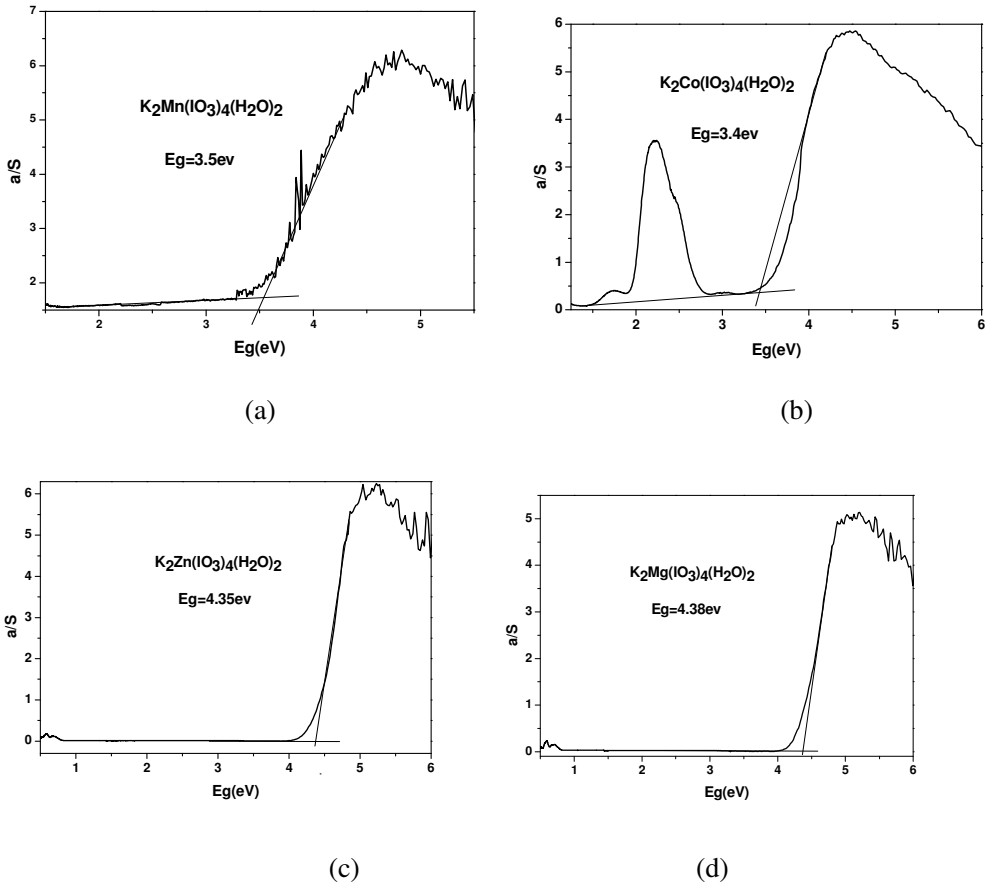


Figure S4. Optical diffuse reflectance spectra for  $K_2\text{M}(\text{IO}_3)_4(\text{H}_2\text{O})_2$  ( $\text{M} = \text{Mn}, \text{Co}, \text{Zn}, \text{Mg}$ ).

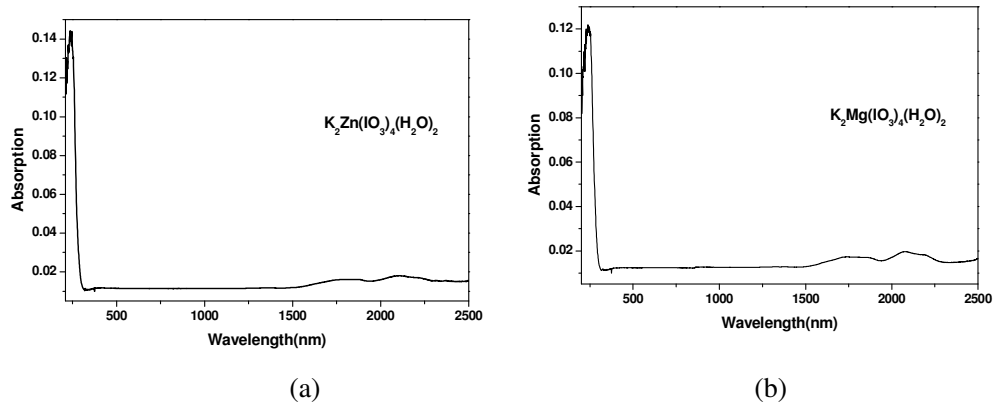


Figure S5. UV absorption spectrum for  $K_2\text{Zn}(\text{IO}_3)_4(\text{H}_2\text{O})_2$  (a) and  $K_2\text{Mg}(\text{IO}_3)_4(\text{H}_2\text{O})_2$  (b).

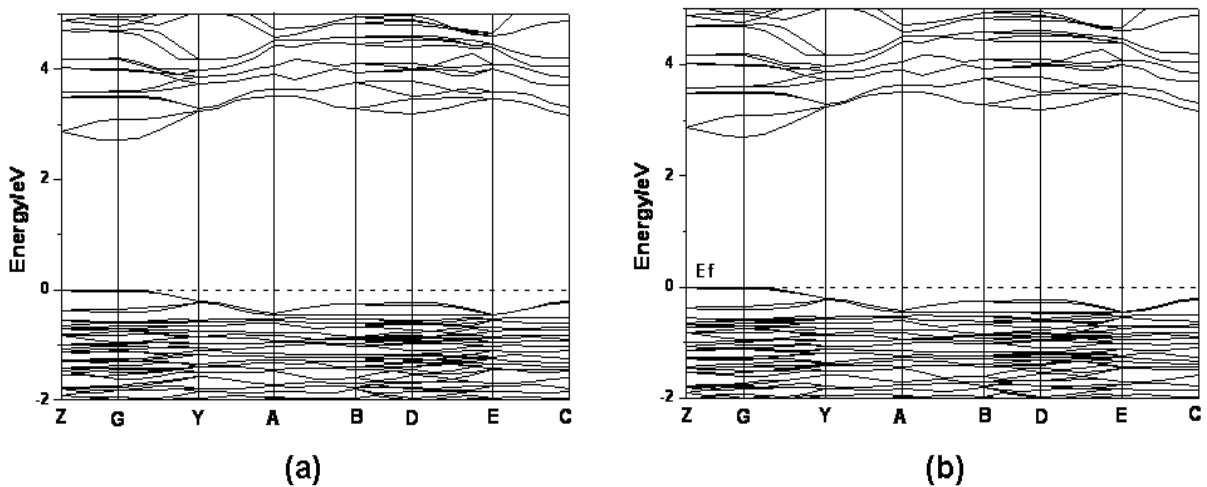
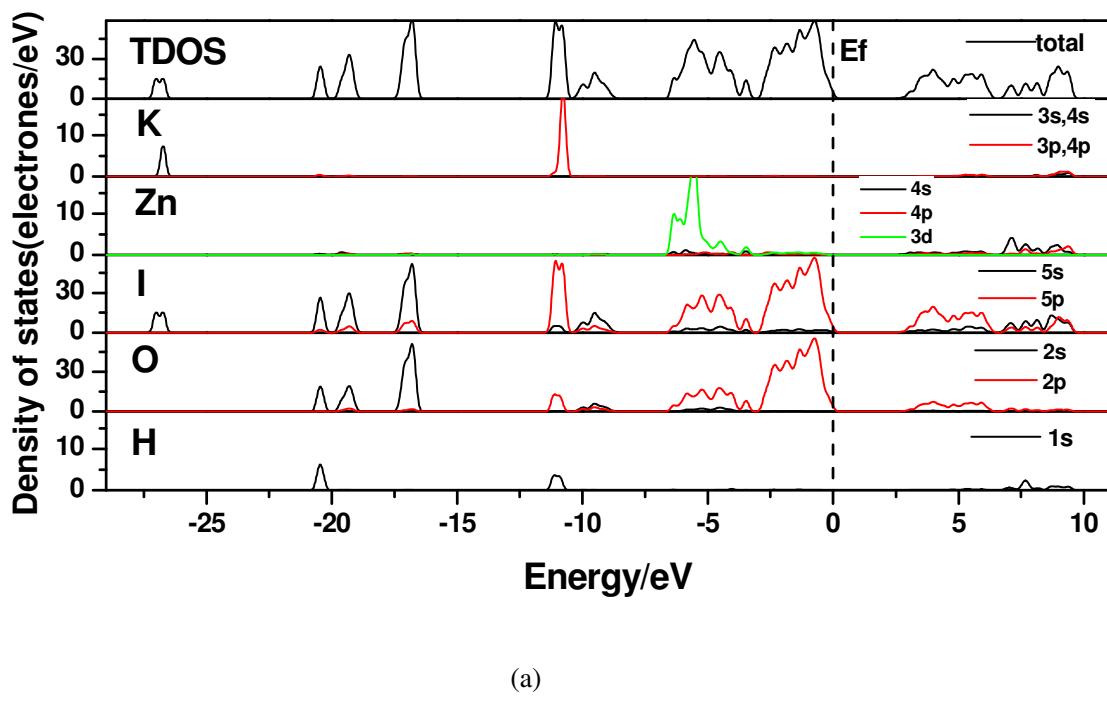
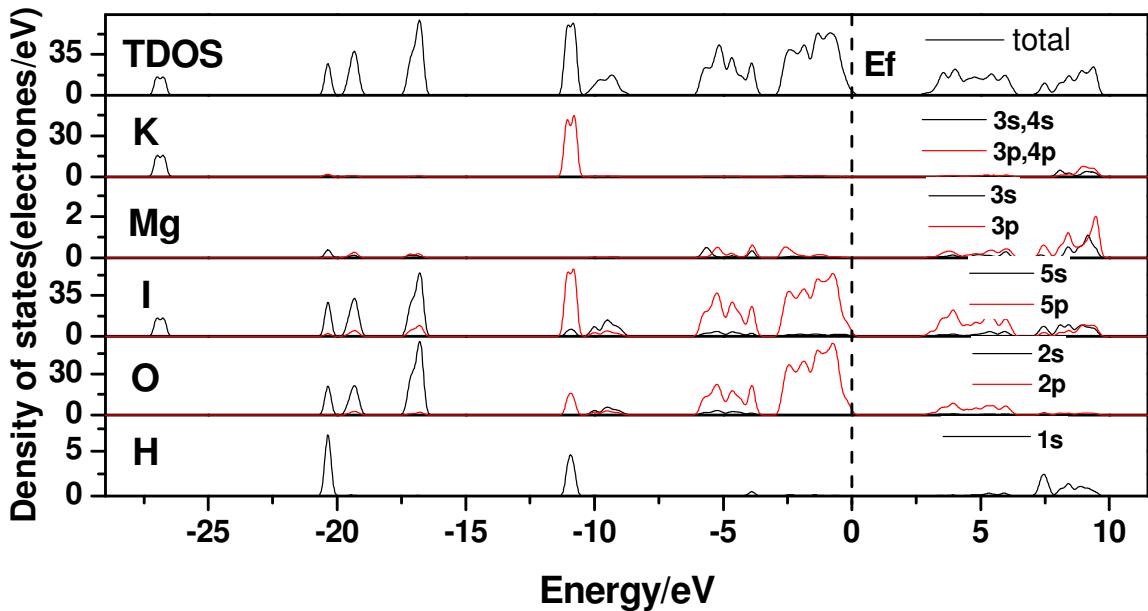


Figure S6. Band structures for  $\text{K}_2\text{Zn}(\text{PO}_4)_4(\text{H}_2\text{O})_2$  (a) and  $\text{K}_2\text{Mg}(\text{PO}_4)_4(\text{H}_2\text{O})_2$  (b). The Fermi level is set at 0 eV.





(b)

Figure S7. Total density of states and partial density of states of  $\text{K}_2\text{Zn}(\text{IO}_3)_4(\text{H}_2\text{O})_2$  (a) and  $\text{K}_2\text{Mg}(\text{IO}_3)_4(\text{H}_2\text{O})_2$ . (b). The Fermi level is set at 0 eV.

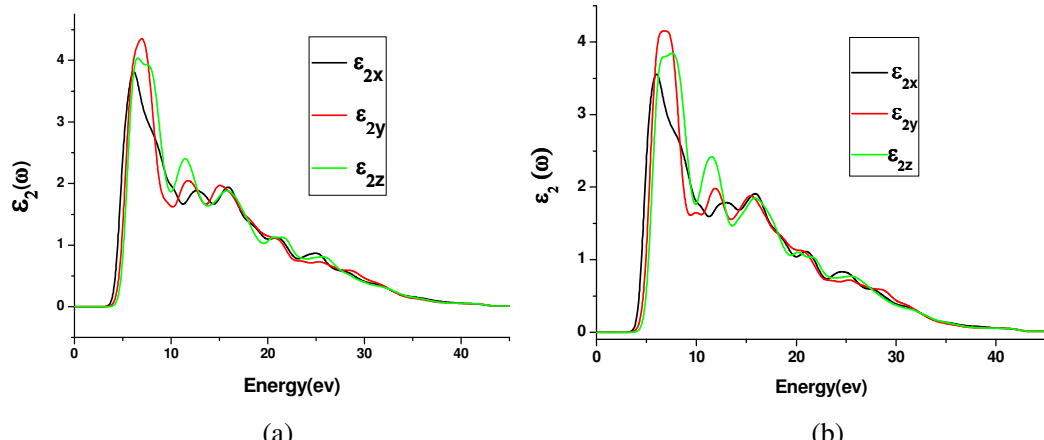


Figure S8. The imaginary part of the dielectric function polarized along three dielectric axial directions and real part of the dielectric function over three dielectric axial directions for  $\text{K}_2\text{Zn}(\text{IO}_3)_4(\text{H}_2\text{O})_2$  (a) and  $\text{K}_2\text{Mg}(\text{IO}_3)_4(\text{H}_2\text{O})_2$  (b).

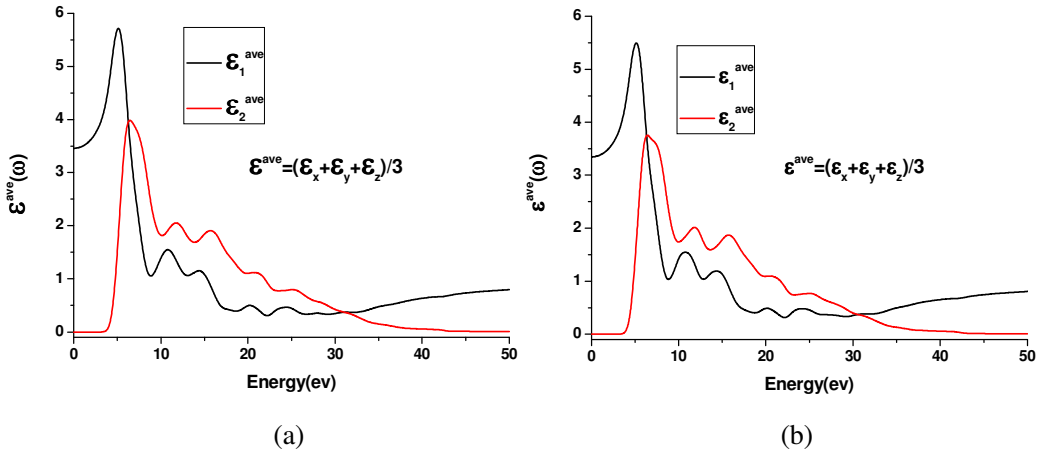


Figure S9. The imaginary part of the dielectric function polarized along three dielectric axial directions and average imaginary part for  $\text{K}_2\text{Zn}(\text{IO}_3)_4(\text{H}_2\text{O})_2$  (a) and  $\text{K}_2\text{Mg}(\text{IO}_3)_4(\text{H}_2\text{O})_2$  (b).

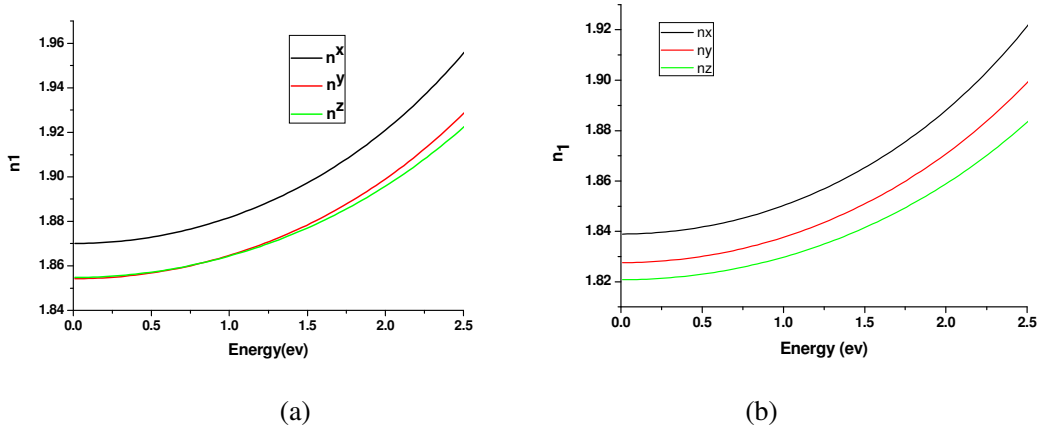


Figure S10. Calculated linear refractive indices for  $\text{K}_2\text{Zn}(\text{IO}_3)_4(\text{H}_2\text{O})_2$  (a) and  $\text{K}_2\text{Mg}(\text{IO}_3)_4(\text{H}_2\text{O})_2$  (b).

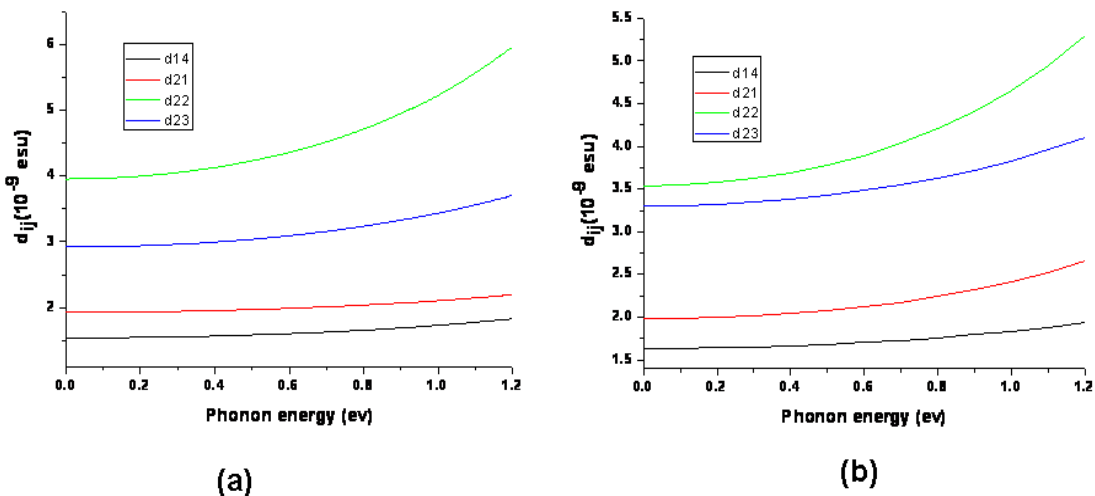


Figure S11. Calculated dynamic second harmonic generation coefficients of  $\text{K}_2\text{Zn}(\text{IO}_3)_4(\text{H}_2\text{O})_2$  (a) and  $\text{K}_2\text{Mg}(\text{IO}_3)_4(\text{H}_2\text{O})_2$  (b).